JOURNAL OF THEORETICAL
AND APPLIED MECHANICS
40, 4, pp. 895-916, Warsaw 2002

TWO-POINT VELOCITY STATISTICS AND THE POD ANALYSIS OF THE NEAR-WALL REGION IN A TURBULENT CHANNEL FLOW

MARTA WACŁAWCZYK
JACEK POZORSKI

Institute of Fluid-Flow Machinery, Polish Academy of Sciences, Gdańsk
e-mail: mw@imp.gda.pl; jp@imp.gda.pl

The Particle Image Velocimetry (PIV) measurements in the near-wall region of a turbulent channel flow have been performed. Two-point velocity statistics are obtained from experimental data and further subjected to the Proper Orthogonal Decomposition (POD) analysis. The resulting empirical function basis characterizes the inhomogeneous shear flow. The first eigenfunction together with spanwise statistics is used in order to find an approximate velocity field of a typical eddy structure.

Key words: near-wall turbulence, PIV, coherent structures, POD analysis

1. Introduction

Great importance of two-point velocity correlations for turbulence analysis arises from the fact that these statistics contain information about vortical structures present in turbulent flows (Pope, 2000). In homogeneous fields the information can be extracted by subjecting two-point correlations to the Fourier analysis (Tennekes and Lumley, 1972) that yields the turbulent energy spectrum. However, most of the technically important flow cases like mixing layers, wakes or wall-bounded flows are strongly inhomogeneous. Numerous experimental observations and DNS computation results indicate the important effect of so-called coherent structures on the flow dynamics (Cantwell, 1981). The coherent structures can be defined as high-energy and high-vorticity regions, often with a typical shape for a given flow case, occurring quite systematically in time and space in contrast to the purely random motion of smaller vortices. In a particular case of near-wall flows, the shapes of

typical coherent structures resemble vortical rolls, elongated in the streamwise direction.

In order to investigate an inhomogeneous turbulent field and detect coherent structures we have to use approaches different than the Fourier analysis. The Proper Orthogonal Decomposition (POD) is a statistical analysis method, based on the two-point correlation functions. It was first introduced to the area of fluid dynamics by Lumley (1970) in order to analyze turbulent flow properties and find an approximate velocity field of coherent structures (Bakewell and Lumley, 1967; Moin and Moser, 1989). The method is a subject of great interest, as it also leads, via the Galerkin projection (Aubry et al., 1988; Panton, 1997), to a low-dimensional set of ordinary differential equations governing the evolution of vortical structures. Solving the equations gives insight into the flow dynamics.

The main aim of the paper is to present POD application to the near-wall region in a turbulent channel flow. Although a detailed POD analysis of the turbulent channel flow has already been performed (Moin and Moser, 1989), it was based on an extensive DNS data set. Here, we carry out the analysis for a set of experimental data. We follow the pioneering paper of Bakewell and Lumley (1967) where the pipe flow was considered. Moreover, we believe that the analysis of the unavoidable PIV measurement error can be another interesting contribution of this paper.

Section 2 presents a short description of the performed PIV experiment. In this Section we also propose a method to estimate the r.m.s. of the PIV error, based on differences between the errors of one- and two-point statistics. This will be also used to reduce a systematic error of the velocity variance. Section 3 contains a concise mathematical description of the POD method. Next, in Section 4 the approach is constrained to the near-wall flow case and is described in a more detailed way, together with some new ideas concerning the derivation of the formula for the velocity field of a coherent structure. Two-point streamwise and wall-normal velocity correlations, together with obtained empirical POD functions, and the resulting typical eddy are presented in Section 5.

2. PIV experiment

Experimental measurements in the wall region of the turbulent channel flow at the Reynolds number (based on the centerline velocity and the channel

half-width) Re = 6600 have been performed with the Particle Image Velocimetry (PIV) technique (Ronald, 1991). In order to carry out the measurement, a thin sheet of the Nd:YAG laser light is directed into the channel, perpendicular to its walls. The CCD Kodak ES 1.0 camera takes two pictures in short time intervals, $\Delta t = 100\,\mu$s, recording the images of seeding particles (here: smoke) injected into the channel. The instantaneous velocity field is computed from the registered particle displacements in the time interval between consecutive snapshots.

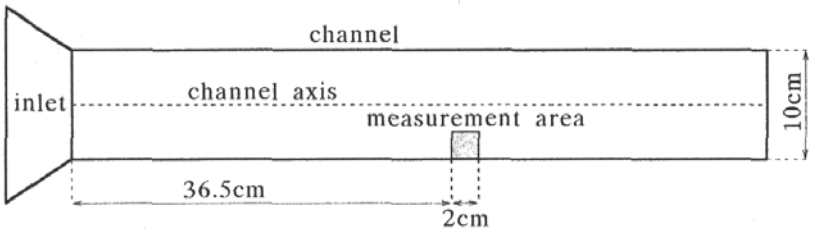

Fig. 1. Flow geometry

The size of the measurement area was $21 \times 21\,\text{mm}^2$. In wall units y^+, it was located in the region $4 \leqslant y^+ \leqslant 130$. The position of the measurement area (cf. Fig. 1) indicates that the flow has not yet reached the state of full development in the whole channel cross-section. However, we do not think that this is of major importance for the subsequent POD analysis that refers to the near-wall region, $y^+ \leqslant 60$. From the experiment, 100 pictures of the instantaneous velocity field with a spatial resolution of 249×251 samples for each picture have been obtained. Time separation between subsequent pairs of snapshots was sufficiently large so that they could be treated as statistically independent flow realizations. After averaging of the pictures over all realizations, we get a mean streamwise velocity component $\langle U \rangle$. The friction velocity and the von Karman constant deduced from linear and log-law profiles are respectively equal to $u_* = 0.09\,\text{m/s}$ and $\kappa = 0.46$.

Next, turbulence statistics like the streamwise velocity variance $\langle u^2 \rangle$ are computed (Fig. 2). Two-point statistics have been obtained by averaging the products of velocity fluctuation measured at two different points of the flow $Q(x_1, y_1; x_2, y_2) = \langle u(x_1, y_1) u(x_2, y_2) \rangle$. The correlations will be used in the subsequent considerations.

2.1. Error estimation

The PIV measurement error of instantaneous velocity arises from non-uniform distribution of seeding particles as well as from errors in particle

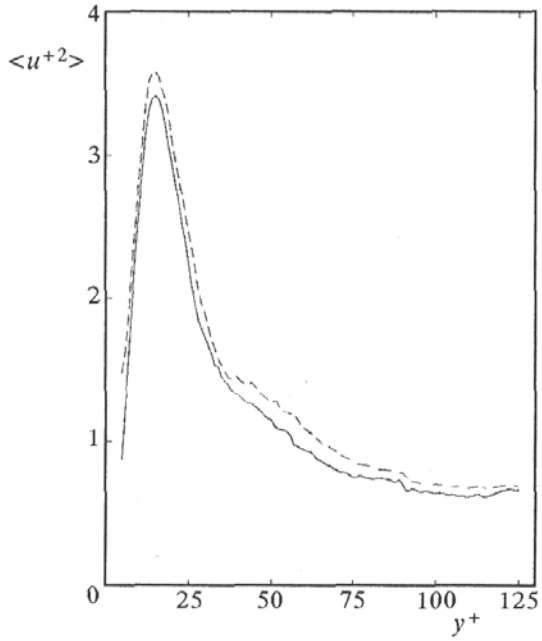

Fig. 2. Variance of the streamwise velocity fluctuation; computed (– – –), corrected (——)

displacement estimations. More precisely, it is related to the PIV algorithm of computing the instantaneous velocity at a point by smoothing the data from neighboring space locations; Westerweel (2000) provides an example of the PIV error analysis. It is related to the measurement error of instantaneous particle displacement. Following Willert and Gharib (1991), we assume here that the error can be treated as approximately Gaussian. In the following considerations we show how to estimate its standard deviation σ_Δ from the comparison between the computed one- and two-point turbulence statistics. This derivation is presented in detail in the Appendix. In turbulent flows, instantaneous velocity consists of its mean and fluctuation part. Assuming that the fluctuations are Gaussian and taking into account the Gaussian error, the measured instantaneous velocity U of a given flow realization can be written as

$$U = \langle U \rangle + u + \sigma_\Delta \xi_\Delta = \langle U \rangle + \sigma_u \xi_u + \sigma_\Delta \xi_\Delta \tag{2.1}$$

where σ_u is the r.m.s. of the velocity fluctuation and σ_Δ is the standard deviation of the measurement error; ξ_u, ξ_Δ are independent standard Gaussian numbers. In practice, the mean velocity $\langle U \rangle$ is obtained by averaging the measured velocity U over N independent realizations. Next, we have computed the fluctuation field by subtracting the mean velocity field from an instantaneous one. This leads to the expression for the error of the velocity fluctuation u

and the error of its square u^2 (see Appendix). After averaging over N realizations the computed $\langle u^2 \rangle$ statistic can be written as

$$\langle u^2 \rangle_{comp} = \sigma_u^2 + \sigma_\Delta^2 + \sqrt{\frac{2}{N}} \sqrt{\sigma_\Delta^4 + 2\sigma_\Delta^2 \sigma_u^2}\, \xi \tag{2.2}$$

With $N = 100$ realizations and after averaging over uncorrelated points in the streamwise direction the last term in the above equation is relatively small. However, there is still the systematic error σ_Δ^2 that increases the computed fluctuation variance and is independent of the number of realizations N. Knowing σ_Δ^2 we could subtract it from the computed velocity variance and obtain a more accurate value. For this purpose we will consider the errors of two-point statistics. This will be more complicated, since for small space intervals the measurement errors, i.e. the random variables ξ_Δ at two different points are correlated. Denoting the space interval between the two points by r, for $r \to 0$ we obtain formula (2.2). On the other hand, in large r limit the computed two-point statistics can be written as

$$\begin{aligned} \langle u(x)u(x+r) \rangle_{comp} &= \langle u(x)u(x+r) \rangle + \\ &+ \frac{1}{\sqrt{N}} \sqrt{\sigma_{\Delta 1}^2 \sigma_{\Delta 2}^2 + \sigma_{\Delta 1}^2 \sigma_{u2}^2 + \sigma_{\Delta 2}^2 \sigma_{u1}^2}\, \xi \end{aligned} \tag{2.3}$$

where $\sigma_{\Delta 1}$, $\sigma_{\Delta 2}$, σ_{u1}, σ_{u2} are the error and fluctuation standard deviations at the points x and $x+r$, respectively, and $\langle u(x)u(x+r) \rangle$ is the exact two-point correlation value.

The conclusion is that the error of two-point correlation decreases with the increasing r value. This can be clearly seen in Fig. 3. For small r (say $r^+ < 5$) the slopes of two-point streamwise statistics are very steep, in this region we observe peaks that do not occur in accurate turbulence statistics. Outside this interval, random errors at two different points are not correlated. From the comparison of (2.2) with (2.3), the variances σ_Δ^2 as well as their correlations can be calculated out of the two-point statistics. The variances are equal to the heights of peaks (Fig. 3). We have found that σ_Δ increases with decreasing distance to the wall, from 1% of the largest mean velocity value in the measurement area at $y^+ = 130$ to 3% at $y^+ = 4$, i.e. the uncertainty of a single velocity measurement changes from 2 to 6%. The errors are correlated within about 5 measurement points (roughly 2 wall units). Figure 2 presents the computed velocity variance and the one corrected by subtracting σ_Δ^2. The maximum r.m.s. error of $\langle u^2 \rangle$ in the buffer and logarithmic layer attains 4% (the uncertainty equals 8%). The largest uncertainty for

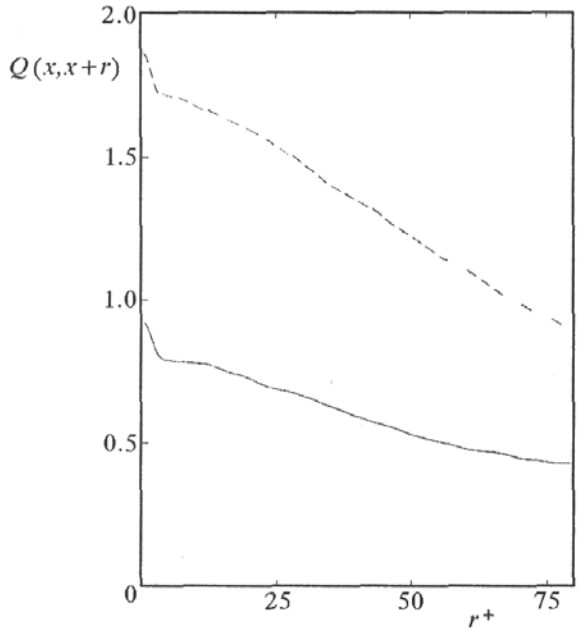

Fig. 3. Two-point streamwise correlations at $y^+ = 15$ (– – –), $y^+ = 35$ (——)

streamwise two-point correlations occurs on the tails of the curves, as they are not averaged in the streamwise direction, its value is approximately equal to ± 0.07. The one for wall-normal statistics (and for the resulting eigenfunctions) does not exceed ± 0.02.

3. Mathematical formulation of POD

The Proper Orthogonal Decomposition is a method of random field analysis, which leads to the empirical function basis, optimal for the energy representation (Aubry, 1991; Berkooz et al., 1993; Holmes et al., 1996). The basis is not given analytically but is determined from experimental or numerical data of two-point correlations of the velocity field. We note that the optimality of the basis relates to coherent structures which can be defined as high-energy regions. This makes us expect that using the POD method one can find the velocity field of coherent structures. As we feel that the issue is only tersely addressed in most of recent articles, we present here, at some detail, the mathematical formulation of the problem and show how the two-point statistics are involved into the considerations.

The mathematical concept of the Proper Orthogonal Decomposition (Lumley, 1970) is based on the assumption that a given velocity component $u_\omega(x)$ of a turbulent field realization ω can be expressed as a linear combination of orthogonal functions $\phi^{(k)}(x)$ with random and statistically independent coefficients $a_\omega^{(k)}$

$$u_\omega(x) = \sum_{k=1}^{\infty} a_\omega^{(k)} \phi^{(k)}(x) \tag{3.1}$$

where

$$\begin{aligned} a_\omega^{(k)} &= \left(u_\omega, \phi^{(k)*}\right) = \int_\Omega u_\omega(x)\phi^{(k)}(x)\, dx \\ \left(\phi^{(k)}(x), \phi^{(l)}(x)\right) &= \int_\Omega \phi^{(k)}(x)\phi^{(l)*}(x)\, dx = \delta_{kl} \end{aligned} \tag{3.2}$$

the parenthesis $(\cdot,\cdot)$ denotes a scalar product of functions; x could be either the position vector or any spatial or temporal coordinate; Ω is the flow area, $*$ denotes the complex conjugate and δ_{kl} is the Kronecker delta.

The most important property of the POD method is expressed by the fact that the function basis $\{\phi^{(k)}(x)\}$ is not given *a priori* (eg. as the Fourier sines and cosines basis), but is deduced from two-point correlation data. The expression $\langle (a_\omega^{(k)})^2 \rangle$ represents the average energy of the kth POD mode. We want the basis to be optimal in the energy representation, i.e. we seek for functions $\phi^{(k)}$, for which the expression

$$\frac{\left\langle \left(u_\omega, \phi^{(k)}\right)\left(u_\omega, \phi^{(k)}\right)^* \right\rangle}{(\phi^{(k)}, \phi^{(k)})} = \left\langle (a_\omega^{(k)})^2 \right\rangle = \lambda^{(k)} \tag{3.3}$$

reaches its maximum value (the Einstein sum convention does not apply here). In further considerations the index (k) is skipped. Defining the average $\langle\cdot\rangle$ as a sum over N realizations, formula (3.3) is written as follows

$$\begin{aligned} \lambda(\phi(x), \phi(x)) &= \frac{1}{N} \sum_{\omega=1}^{N} \int_\Omega u_\omega(x)\phi^*(x)\, dx \int_\Omega u_\omega^*(x')\phi(x')\, dx' = \\ &= \int_\Omega \int_\Omega \Big[\frac{1}{N} \sum_{\omega=1}^{N} u_\omega(x) u_\omega^*(x')\Big] \phi^*(x)\phi(x')\, dx dx' \end{aligned} \tag{3.4}$$

The expression in brackets is the two-point correlation function $Q(x, x')$. Next, the variational method (Lumley, 1970) is used in order to find the maximum value of λ, which leads to the eigenfunction and eigenvalue problem

$$\Big(Q(x, x'), \phi^*(x')\Big) = \lambda\phi(x) \tag{3.5}$$

The solution to (3.5) gives a class of functions $\phi^{(k)}(x)$ which form, for a given flow case, the optimal POD basis. In homogeneous and isotropic turbulent fields the two-point correlation function depends only on the difference $x - x'$ and can be therefore expressed as the Fourier series

$$Q(x, x') = \sum_{k=1}^{\infty} C_k \exp[\mathrm{i}k(x - x')] = \sum_{k=1}^{\infty} C_k \exp(\mathrm{i}kx) \exp(-\mathrm{i}kx') \tag{3.6}$$

Using the above formula in equation (3.5) we find that $\{\exp(\mathrm{i}kx)\}$ constitute the eigenfunction basis with eigenvalues C_k. The conclusion is that for homogeneous velocity fields (at least in one direction) the Fourier sine and cosine functions are the optimal basis and therefore the Fourier analysis is an appropriate method for examining these fields.

4. POD for the near-wall region of a channel flow

In this section we present the application of the POD method to a particular case of the near-wall region of the channel flow and derive the expression for the velocity field of a typical eddy structure. Since the flow is homogeneous in the streamwise and spanwise directions (x and z), the fluctuation field can be expressed as

$$u_\omega(x, y, z) = \sum_{k=1}^{\infty} a_\omega^{(k)}(x, z)\phi^{(k)}(y) \tag{4.1}$$

where $\{\phi(y)\}$ are eigenfunctions, and $a_\omega^{(k)}$ denotes their random coefficients. From normalization condition (3.2) and from (4.1), the two-point correlation function has the form

$$\begin{aligned} &Q(x, x'; y, y'; z, z') = Q(r_x; y, y'; r_z) = \\ &= \sum_{k=1}^{\infty} \Big\langle a_\omega^{(k)}(x, z) a_\omega^{(k)}(x', z') \Big\rangle \phi^{(k)}(y)\phi^{(k)}(y') \end{aligned} \tag{4.2}$$

where $r_x = x - x'$, $r_z = z - z'$. In order to obtain the optimal basis $\{\phi\}$, eigenvalue problem (3.5) has to be solved in the wall-normal direction. If we assume $r_x = 0$ and $r_z = 0$, then

$$\int_0^{L_y} Q(y, y')\phi(y')\, dy' = \lambda\phi(y) \tag{4.3}$$

where $Q(y, y') = Q(0; y, y'; 0)$ and L_y is the height of the measurement area. The resulting eigenfunctions $\phi^{(k)}(y)$ with the eigenvalues $\lambda^{(k)} = \langle (a_\omega^{(k)}(0,0))^2 \rangle$ contain information about the fluctuation field; also, a qualitative velocity field of the coherent structure can be deduced out of them.

For this purpose we will use two additional assumptions (Bakewell and Lumley, 1967). In formula (4.2) we neglect all functions except the first one, which relates to the highest eigenvalue, as it contains the major part of the fluctuation field energy. The two-point correlation function can be then expressed as the inverse Fourier transform

$$Q(r_x; y, y'; r_z) \approx \phi^{(1)}(y)\phi^{(1)}(y')\mathcal{F}^{-1}[H(k_x, k_z)] \tag{4.4}$$

where $H(k_x, k_z)$ is the Fourier transform of $\langle a^{(1)}(x, z)a^{(1)}(x', z') \rangle$ in homogeneous directions x and z. Henceforth, the index (1) will be neglected.

The second assumption is concerned with a stochastic process which scatters coherent structures in the (x, z) plane. Let $\Psi(x - x_{n\omega}, y, z - z_{n\omega})$ be a component of the velocity field of a structure; the point $(x_{n\omega}, z_{n\omega})$ fixes its position in space. The function Ψ has a compact support (i.e. its value equals 0 apart from the bounded area) and is an even function of its arguments x and z. We assume that coherent structures positions $(x_{n\omega}, z_{n\omega})$ and their amplitudes $a_{n\omega}$ are random and statistically independent. In other words, the functions $\Psi(x, y, z)$ are scattered in the (x, z) plane by a stochastic process g_ω

$$g_\omega(x, z) = \sum_{n=1}^{N} a_{n\omega}\delta(x - x_{n\omega}, z - z_{n\omega}) \tag{4.5}$$

As the flow is dominated by the largest eigenfunctions, we further assume that the fluctuation field contains only the coherent structures characterized by the function Ψ. The situation for the one dimensional case is presented in Fig. 4. The fluctuation field u can be therefore written as a convolution of the function Ψ and the process g

$$u_\omega(x, y, z) = \iint \Psi(x - x'', y, z - z'')g_\omega(x'', z'')\, dx''dz'' \tag{4.6}$$

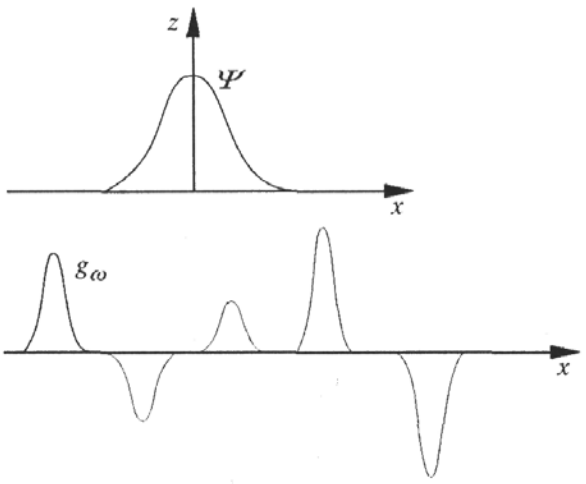

Fig. 4. Schematic "coherent structure" ψ and its convolution with g_ω

The two-point correlation function has the following form:

$$\langle u(x,y,z)u(x',y',z')\rangle = \iiiint \Psi(x-x'',y,z-z'')\Psi(x'-x''',y',z'-z''')\cdot \cdot\langle g(x'',z'')g(x''',z''')\rangle\, dx''dz''dx'''dz''' \tag{4.7}$$

Basing on equation (4.5), the expression for two-point correlations of g is

$$\langle g(x,z)g(x',z')\rangle = \delta(x-x',z-z') \tag{4.8}$$

Using the above relation in (4.7) and comparing with (4.4), for the case $y = y'$ we obtain

$$\phi^2(y)\mathcal{F}^{-1}[H(k_x,k_z)] = \iint \Psi(\xi,y,\zeta)\Psi(\xi-r_x,y,\zeta-r_z)\, d\xi d\zeta \tag{4.9}$$

where $\xi = x - x''$, $\zeta = z - z''$. As we have previously assumed, Ψ is an even function of its first and third argument. So, after the Fourier transform in the x and z directions, the RHS of the above equation will contain the Fourier transform of the convolution of the functions Ψ that is further expressed as the product of Fourier's transforms. Finally, the velocity field of the coherent structure can be written as

$$\Psi(r_x,y,r_z) \approx \pm\phi(y)\mathcal{F}^{-1}[H^{1/2}(k_x,k_z)] = \pm\phi(y)F(r_x,r_z) \tag{4.10}$$

Note that we do not have any information about the phase, or in other words – about the structures positions in the (x,z) plane. This information has been lost because the fluctuation field is homogeneous in the x and z directions.

5. Eigenfunctions of the turbulent channel flow

5.1. Two-point correlations in homogeneous directions

Based on experimental data, the two-point correlations of the u velocity component have been obtained in the area perpendicular to the channel wall. Figure 5 presents two-point correlations in the streamwise direction $Q(r_x; y = y'; 0)$. It can be seen that for a certain y^+ range $(5 \leqslant y^+ \leqslant 25)$ the fluctuation field is strongly correlated. This fact confirms the existence of the mentioned coherent roll structures, elongated in the flow direction.

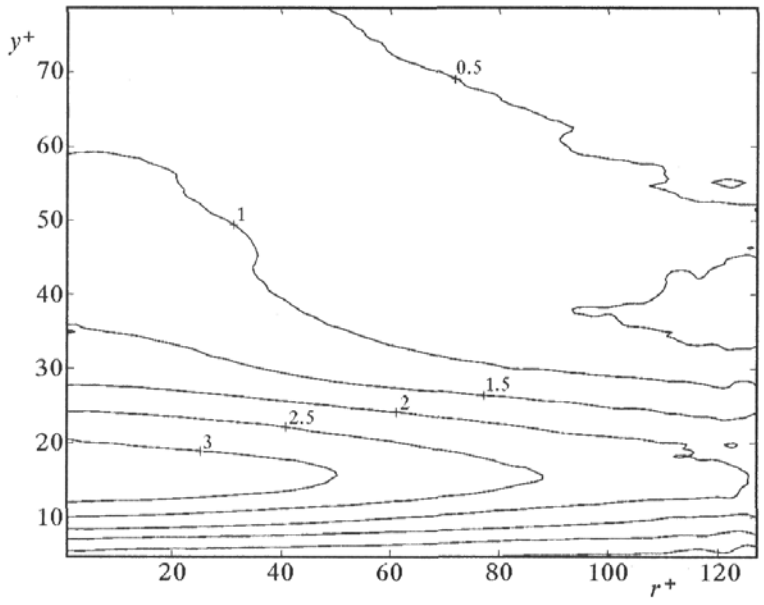

Fig. 5. Two-point streamwise correlation

The spanwise statistics change their sign for bigger r_z values. This is a typical feature of a cross-correlation function in a homogeneous direction. The spanwise statistic presented in Fig. 6 is taken from the DNS computation (Kim et al., 1987) of fully developed turbulent channel flow. It will be used in further considerations because of the lack of PIV data in the spanwise direction.

5.2. Eigenfunctions in the y direction

Two-point correlation in wall-normal direction $Q(y, y')$ is presented in Fig. 7. Since the wall-normal direction is inhomogeneous, the two-point correlations depend on both arguments y and y' separately, and not on their difference $y - y'$. In Fig. 7, the velocity variance $\langle u^2 \rangle$ is readily found on the

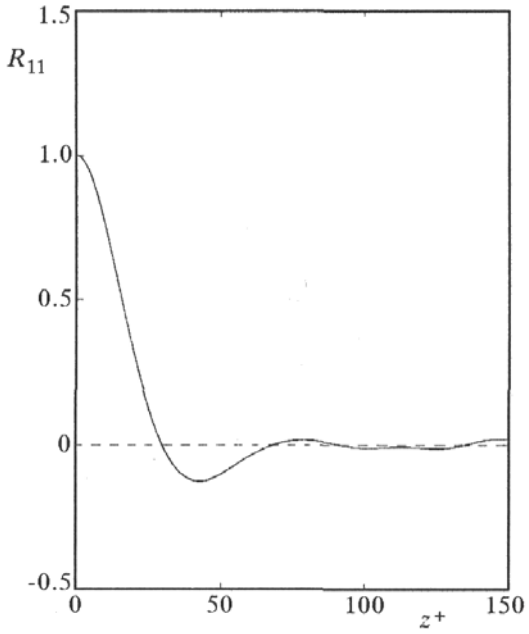

Fig. 6. Two-point spanwise correlation coefficient at $y^+ = 5$ (after Kim et al. (1987))

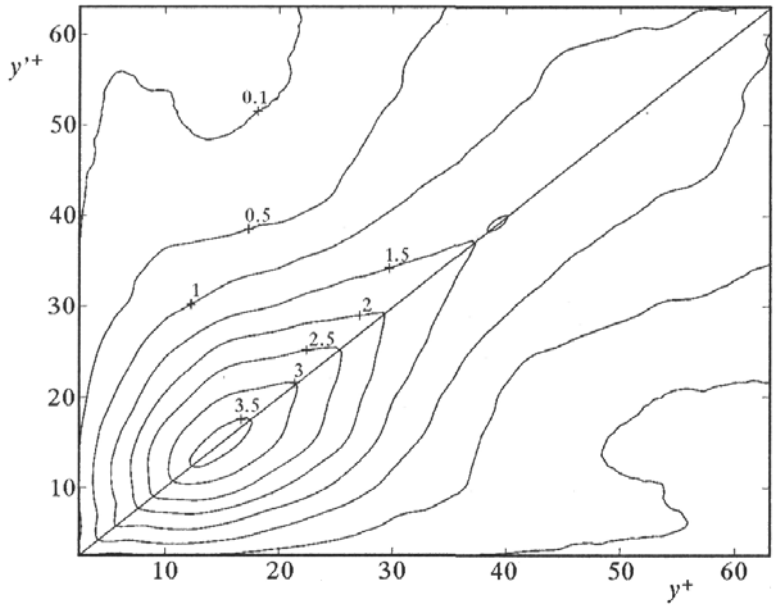

Fig. 7. Two-point correlation in the wall-normal direction

diagonal line $y = y'$. This wall-normal correlation has been used in equation (4.3) in order to compute the near-wall eigenfunctions out of it.

Eigenvalue problem (4.3) has been solved by the standard Inverse Iteration method (Press et al., 1992), which is optimal for this case, as we need only a few eigenfunctions with the largest eigenvalues. The first four of them are presented in Fig. 8. The shapes of subsequent eigenfunctions are increasingly closer to the *sine* function. As was already mentioned, the Fourier *sine* and *cosine* basis is optimal for the homogeneous field. The conclusion is that a few first eigenfunctions describe the flow inhomogeneity, since the subsequent ones are typical for homogeneous flows.

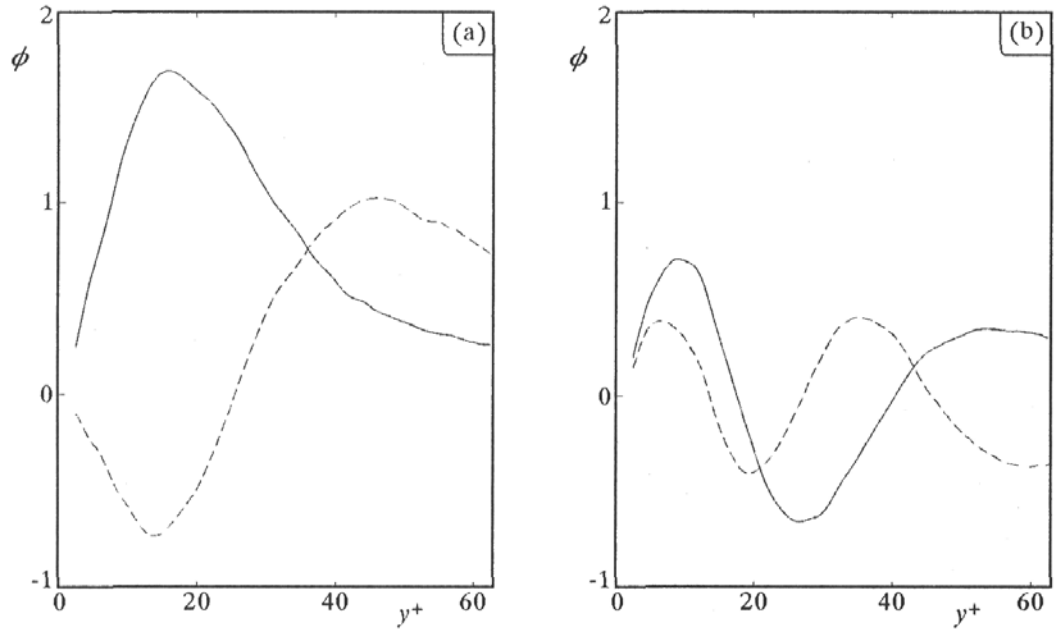

Fig. 8. Eigenfunctions: (a) first (——), second (– – –), (b) third (——), fourth (– – –)

For $r_x = 0$ and $r_z = 0$, setting $y = y'$ in equation (4.2), we obtain the u-fluctuation variance as a function of the wall distance

$$\langle u^2(y) \rangle = \sum_{n=1}^{\infty} \lambda_n \phi_n^2(y) \tag{5.1}$$

Figure 9 presents the sums of 1, 2, 3 and 4 squares of the eigenfunctions, respectively. The comparison with the fluctuation variance confirms the POD basis optimality in the energy representation.

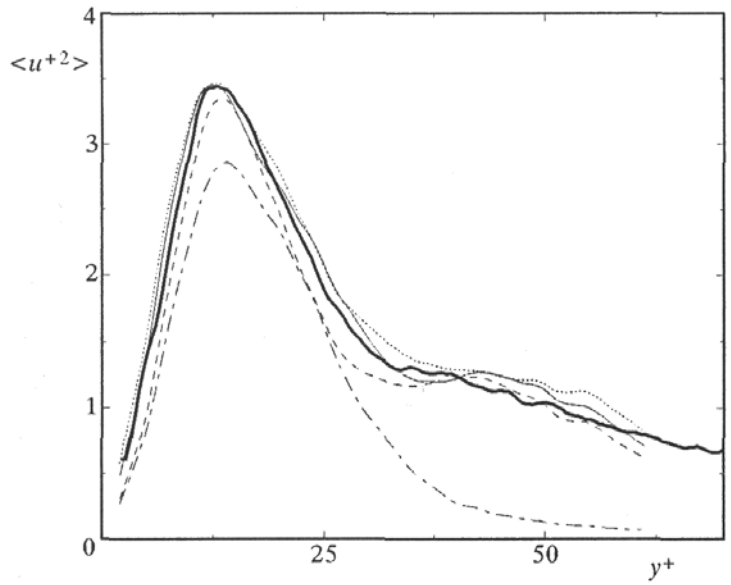

Fig. 9. Fluctuation variance (bold line) and sums of squares of eigenfunctions: 1 (– · – · –), 2 (– – –), 3 (· · · ·) , 4 (——)

5.3. Velocity field of coherent structures

From the PIV experiment we have obtained only u-component statistics. In order to obtain an approximate velocity field of a coherent structure we need to introduce some additional simplifications. From the negative correlation of u and v in the near-wall region we assume that $v \sim -u$. Using equation (4.10) for u-fluctuation we obtain

$$\begin{aligned} u &\approx -\Psi(r_x, y, r_z) = -\phi(y)F(r_x, r_z) \\ v &\sim \Psi(r_x, y, r_z) = \phi(y)F(r_x, r_z) \end{aligned} \tag{5.2}$$

The w-fluctuation component can be found from the continuity equation

$$\frac{\partial u}{\partial x} + \frac{\partial v}{\partial y} + \frac{\partial w}{\partial z} = 0 \tag{5.3}$$

Taking into account the big streamwise correlation of the vortical structures (Fig. 5), for small r_x we can assume

$$\frac{\partial u}{\partial x} \approx 0 \qquad w(y,z) \approx -\int_0^z \frac{\partial v(y,z)}{\partial y}\, dz \tag{5.4}$$

Finally, the velocity field of the coherent structure in the (y, z) plane is obtained from the following equations

$$v^+(y, r_z^+) \sim \phi(y^+) F(0, r_z^+)$$
$$w^+(y, r_z^+) \sim \frac{\partial \phi(y^+)}{\partial y^+} \int_0^{r_z^+} F(0, r_z^+)\, dr_z^+ \tag{5.5}$$

Figure 10 presents the resulting streamlines of the coherent structure in the (y, z) plane. It forms two counter-rotating rolls placed in the area of high streamwise correlations $(5 \leqslant y^+ \leqslant 25)$, which means that they are elongated in the flow direction. The similar roll shape was obtained by other authors from POD analysis (Bakewell and Lumley, 1967; Moin and Moser, 1989) and from conditional sampling techniques. Different visualisation techniques confirm the presence of many elongated vortical structures in the near-wall turbulence field (Cantwell, 1981; Robinson, 1991).

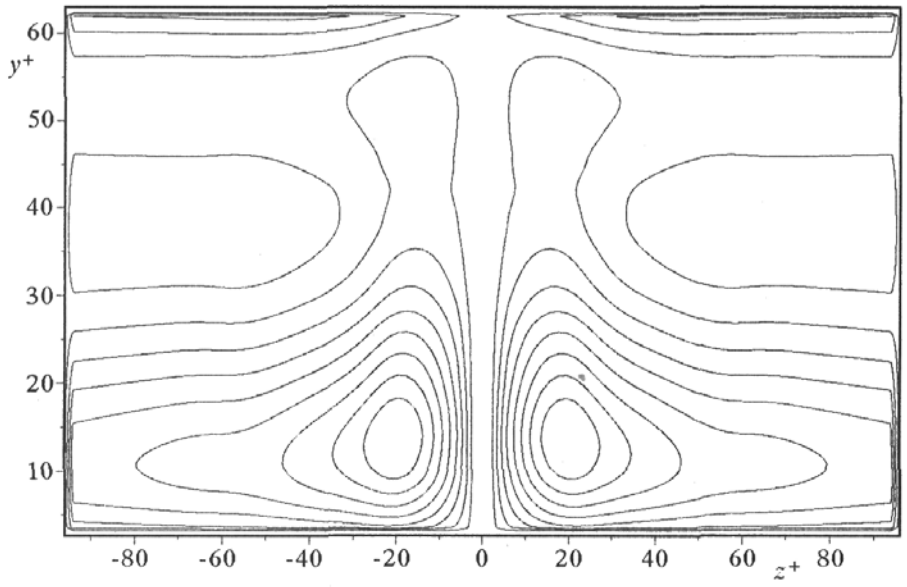

Fig. 10. Coherent structure in the near-wall region: streamlines

6. Conclusions

6.1. Summary

In the paper we have presented velocity statistics obtained from the PIV experiment together with ample discussion of the measurement error. The latter is particularly important when strong velocity gradients occur within the PIV measurement area like in the case for near-wall flows. The POD analysis of two-point correlations enabled us to find the empirical basis, where the first and second eigenfunctions were dominating and the following functions shapes resembled more and more the ones characteristic for homogeneous flows. That is the reason to suppose that only a few first eigenfunctions describe the flow inhomogeneity. The obtained streamwise statistics show large correlations in a certain range of wall-distances ($5 \leqslant y^+ \leqslant 25$) which indicates the existence of elongated structures in the fluctuation field. The computed first eigenfunction and spanwise flow statistics from (Kim et al., 1987) were used in order to find the velocity field of a typical eddy structure. This confirms the fact that two-point statistics contain information about vortical structures present in the flow.

6.2. Limitations and future development

Figure 11 presents the coherent structure resulting from the two-point correlation analysis superposed with the schematic picture of hairpin vortices in an instantaneous fluctuation field. It can be seen that the analysis of averaged statistics gives only an "approximate" or "typical" eddy which is not the instantaneous picture of the flow. We argue that a suitable averaging of the velocity induced by hairpin vortices results in the mean structure (streamwise rolls), as the contributions of the hairpin "head" (central region) compensate each other, but those of the "arms" inclined to the (x, z) plane add to the velocity components in the (y, z) plane, finally resulting in averaged rolls. The experimental analysis of turbulent near-wall regions shows that the so-called "bursting events", caused by a sudden breaking of vortical rolls, contain large energy contribution and strongly influence the flow dynamics. However, the POD method uses the averaged correlation functions, so the energetic but rare events like "bursts" are lost during the averaging process. In order to describe the rare structures, methods of the single flow realization analysis, like the wavelet technique, are needed (Farge, 1992). Such an analysis of the PIV experimental data has been also performed by the authors (Wacławczyk and Pozorski, 2002).

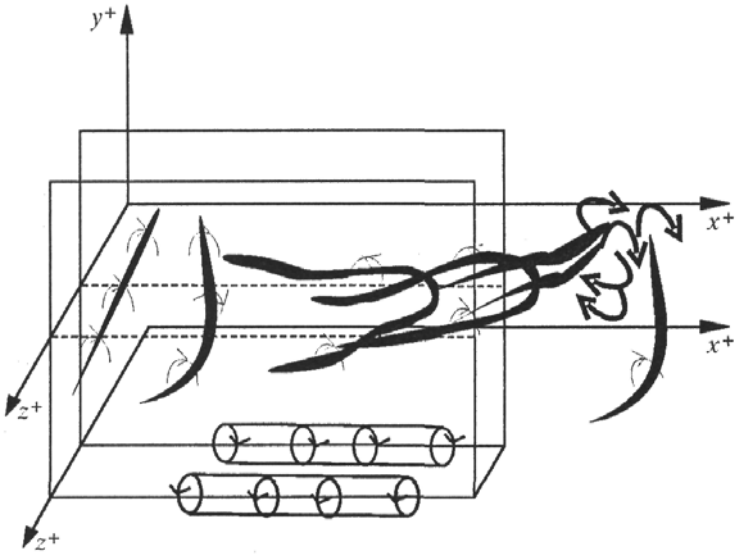

Fig. 11. Coherent structure in the near-wall region: streamlines

All the above considerations concern only the kinematical point of view. The next step is to study the dynamics of the coherent structures. This can be attempted by projecting the truncated function basis on the governing equations (Aubry et al., 1988; Holmes et al., 1996; Joia et al., 1998); the resulting set of ordinary differential equation constitutes a low-dimensional turbulence model, arguably well-suited for low-cost simulations of flows dominated by distinct vortical structures and for turbulence control. The model can also be used to investigate the near-wall transport of passive scalars (eg. heat transfer), which additionally confirms the technical importance of the above analysis.

Acknowledgement

Substantial help of J. Dekowski (Department of Applications of Plasma and Laser Techniques, IMP PAN Gdańsk) in the acquisition of experimental data is gratefully acknowledged.

A. Appendix

In turbulent flows an instantaneous velocity consists of its mean and fluctuation part. Assuming that the fluctuation is Gaussian and taking into account the Gaussian error, the measured instantaneous velocity can be written as

$$U = \langle U \rangle + u + \sigma_\Delta \xi_\Delta = \langle U \rangle + \sigma_u \xi_u + \sigma_\Delta \xi_\Delta \tag{A.1}$$

where σ_u and σ_Δ are the r.m.s. of the velocity fluctuation and the standard deviation of the measurement error, respectively; ξ_u, ξ_Δ are the independent Gaussian random numbers of zero mean values and the variances $\langle \xi_u^2 \rangle = \langle \xi_\Delta^2 \rangle = 1$. The mean velocity field is computed by averaging the measured velocity U over N independent realizations. In the limit $N \to \infty$

$$\lim_{N\to\infty} \frac{1}{N} \sum_{n=1}^{N} U^{(n)} = \langle U \rangle \tag{A.2}$$

but since the number of realizations is finite, it can be found from (A.1) and (A.2) that the mean velocity value has a Gaussian error with a standard deviation σ_Σ that for large N goes to 0 as $1/\sqrt{N}$

$$\sigma_\Sigma = \sqrt{\left\langle \left(\frac{1}{N} \sum_{n=1}^{N} U^{(n)} - \langle U \rangle \right)^2 \right\rangle} = \frac{1}{\sqrt{N}} \sqrt{\sigma_u^2 + \sigma_\Delta^2} \tag{A.3}$$

The fluctuation field is computed by subtracting the mean velocity field from the instantaneous one

$$u_{comp}^{(n)} = U^{(n)} - \frac{1}{N} \sum_{n=1}^{N} U^{(n)} = \sigma_u \xi_u^{(n)} + \sigma_\Delta \xi_\Delta^{(n)} - \sigma_\Sigma \xi_\Sigma^{(n)} \tag{A.4}$$

where $u^{(n)} = \sigma_u \xi_u^{(n)}$ is the exact fluctuation value in a given flow realization. Hence, the error of the fluctuation measurement is equal to

$$\Delta_u^{(n)} = \sigma_\Delta \xi_\Delta^{(n)} - \sigma_\Sigma \xi_\Sigma^{(n)} \tag{A.5}$$

The last term in the above equation can be neglected as it is already of order $1/\sqrt{N}$. Now, we want to estimate the r.m.s. error σ_2 of $\langle u^2 \rangle$. The error $\Delta_2^{(n)}$ for a single flow realization n can be obtained from (A.4). After averaging over N realizations

$$\frac{1}{N} \sum_{n=1}^{N} \Delta_2^{(n)} = \sigma_\Delta^2 \frac{1}{N} \sum_{n=1}^{N} (\xi_\Delta^{(n)})^2 + 2\sigma_\Delta \sigma_u \frac{1}{N} \sum_{n=1}^{N} \xi_\Delta^{(n)} \xi_u^{(n)} \tag{A.6}$$

It must be noted that with $N \to \infty$ the above error takes the constant positive value σ_Δ^2. What goes to 0 in large N limit is the variance of the error

$$\begin{aligned} \sigma_2^2 = \left\langle \left(\frac{1}{N} \sum_{n=1}^{N} \Delta_2^{(n)} - \sigma_\Delta^2 \right)^2 \right\rangle = \frac{\sigma_\Delta^4}{N^2} \left\langle \left(\sum_{n=1}^{N} (\xi_\Delta^{(n)})^2 \right)^2 \right\rangle + \\ + \frac{4}{N^2} \sigma_\Delta^2 \sigma_u^2 \left\langle \left(\sum_{n=1}^{N} \xi_\Delta^{(n)} \xi_u^{(n)} \right)^2 \right\rangle + \sigma_\Delta^4 - \frac{2\sigma_\Delta^4}{N} \sum_{n=1}^{N} \langle (\xi_\Delta^{(n)})^2 \rangle \end{aligned} \tag{A.7}$$

The above equation can be re-written as

$$\sigma_2^2 = \frac{\sigma_\Delta^4}{N^2}\Big[\sum_{n=1}^{N}\langle(\xi_\Delta^{(n)})^4\rangle + \sum_{n=1}^{N}\sum_{k=1,k\neq n}^{N}\Big\langle(\xi_\Delta^{(n)}\xi_\Delta^{(k)})^2\Big\rangle\Big] + \\ + \frac{4}{N^2}\sigma_\Delta^2\sigma_u^2\sum_{n=1}^{N}\Big\langle(\xi_\Delta^{(n)}\xi_u^{(n)})^2\Big\rangle - \sigma_\Delta^4 \tag{A.8}$$

Remembering that for Gaussian variables $\langle\xi^4\rangle = 3$ and $\langle\xi_\Delta^2\xi_u^2\rangle = 1$, the expression for the computed mean velocity variance writes finally

$$\langle u^2\rangle_{comp} = \langle u^2\rangle + \sigma_\Delta^2 + \sigma_2\xi = \langle u^2\rangle + \sigma_\Delta^2 + \sqrt{\frac{2}{N}}\sqrt{\sigma_\Delta^4 + 2\sigma_\Delta^2\sigma_u^2}\,\xi \tag{A.9}$$

The last term in the above equation tends to 0 as $N \to \infty$; however, there is still a systematic error σ_Δ^2 that increases the computed fluctuation variance and is independent of the number of realizations N.

The procedure leading to expression for the computed two-point statistics is analogous. The starting point is again formula (A.4). The measured velocity fluctuations at two different points are multiplied and averaged over a finite number of realizations. The random variables at two different points are correlated for small space intervals. Denoting the space interval between two points by r, for $r \to 0$ we obtain formula (A.8), and in large r limit the computed two-point statistics can be written as

$$\langle u(x)u(x+r)\rangle_{comp} = \\ = \langle u(x)u(x+r)\rangle + \frac{1}{\sqrt{N}}\sqrt{\sigma_{\Delta1}^2\sigma_{\Delta2}^2 + \sigma_{\Delta1}^2\sigma_{u2}^2 + \sigma_{\Delta2}^2\sigma_{u1}^2}\,\xi \tag{A.10}$$

$\sigma_{\Delta1}$, σ_{u1}, $\sigma_{\Delta2}$, σ_{u2} are the standard deviations of the error and fluctuation at the points x and $x+r$ respectively, $\langle u(x)u(x+r)\rangle$ is the exact two-point correlation value. The computed two-point statistics tend to the exact value when $N \to \infty$, since no systematic errors occur in the above expression.

Notations

$\mathcal{F}$ – two-dimensional Fourier transform
F – inverse Fourier transform of $H^{1/2}$
H – Fourier transform of $\langle a^{(1)}(x,z)a^{(1)}(x',z')\rangle$
N – number of realizations
Q – two-point correlation function
U – streamwise velocity component
a – POD coefficient
g – stochastic process
k – wavenumber
r – space interval between two points
u_* – friction velocity
u – streamwise velocity fluctuation
v – wall-normal velocity fluctuation
w – spanwise velocity fluctuation
x – streamwise coordinate
y – wall-normal coordinate
z – spanwise coordinate

Greek symbols

Ψ – velocity field of coherent structure
δ – Dirac delta
κ – von Karman constant
λ – POD eigenvalue
ξ – Gaussian number
σ – standard deviation
ϕ – POD eigenfunction

Superscripts and subscripts

$*$ – complex conjugate
$+$ – non-dimensional value
ω – realization
Δ – error
(k) – component of the function basis

References

1. AUBRY N., 1991, On the hidden beauty of the proper orthogonal decomposition, *Theoret. Comput. Fluid Dynamics*, **2**, 339-352
2. AUBRY N., HOLMES P., LUMLEY J.L., STONE E., 1988, The dynamics of coherent structures in the wall region of turbulent boundary layer, *J. Fluid Mech.*, **192**, 115-173
3. BAKEWELL H.P., LUMLEY J.L., 1967, Viscous sublayer and adjacent wall region in turbulent pipe flow, *Phys. Fluids*, **10**, 1880-1889
4. BERKOOZ G., HOLMES P., LUMLEY J.L., 1993, The proper orthogonal decomposition in the analysis of turbulent flows, *Annu. Rev. Fluid Mech.*, **25**, 539-571
5. CANTWELL B.J., 1981, Organized motion in turbulent flow, *Annu. Rev. Fluid Mech.*, **13**, 457-515
6. FARGE M., 1992, Wavelet transforms and their applications to turbulence, *Annu. Rev. Fluid Mech.*, **24**, 359-457
7. HOLMES P., LUMLEY J.L., BERKOOZ G., 1996, *Turbulence, Coherent Structures, Dynamical Systems and Symmetry*, Cambridge University Press
8. JOIA I.A., GOBEAU N., USHIJIMA T., PERKINS R.J., 1998, POD study of bubble and particle motion in turbulent channel flow, *International Conference on Multiphase Flow*, June 8-12, Lyon, France
9. KIM J., MOIN P., MOSER R., 1987, Turbulence statistics in fully developed channel flow at low Reynolds number, *J. Fluid Mech.*, **177**, 133-166
10. LUMLEY J.L., 1970, *Stochastic Tools in Turbulence*, Academic Press, New York and London, 57-62
11. MOIN P., MOSER R.D., 1989, Characteristic-eddy decomposition of turbulence in a channel, *J. Fluid Mech.*, **200**, 471-509
12. PANTON R.L., 1997, *Self-Sustaining Mechanisms of Wall Turbulence*, Computational Mechanics Publications, Southampton
13. POPE S.B., 2000, *Turbulent Flows*, Cambridge University Press, 195-215
14. PRESS W.H., TEUKOLSKY S.A., VETTERLING W.T., FLANNERY B.P., 1992, *Numerical recipes in Fortran 77. The art of scientific computing*, Cambridge University Press, New York
15. ROBINSON K.S., 1991, Coherent motions in the turbulent boundary layer, *Annu. Rev. Fluid Mech.*, **25**, 457-475
16. RONALD J.A., 1991, Particle-imaging techniques for experimental fluid mechanics, *Annu. Rev. Fluid Mech.*, **23**, 261-304

17. TENNEKES H., LUMLEY J.L., 1972, *A First Course in Turbulence*, MIT Press, Cambridge, Mass, 248-286

18. WACŁAWCZYK M., POZORSKI J., 2002, Wavelet analysis of near-wall region in turbulent channel flow, *Turbulence*, **8**, (in print)

19. WESTERWEEL J., 2000, Theoretical analysis of the measurement precision in particle image velocimetry, *Exp. Fluids*, **29**, S3-S12, Suppl. S

20. WILLERT C.E., GHARIB M., 1991, Digital particle image velocimetry, *Exp. Fluids*, **10**, 181-193

Wyznaczanie dwupunktowych funkcji korelacyjnych prędkości i analiza POD przepływu turbulentego w obszarze przyściennym kanału płaskiego

Streszczenie

Wykonany został pomiar turbulentnego pola prędkości w obszarze przyściennym kanału płaskiego metodą PIV (ang. *Particle Image Velocimetry*). Na podstawie danych pomiarowych wyznaczono dwupunktowe funkcje korelacyjne prędkości, które następnie poddane zostały analizie POD (ang. *Proper Orthogonal Decomposition*). Otrzymana w wyniku tej analizy baza empirycznych funkcji własnych charakteryzuje niehomogeniczny przepływ w obszarze przyściennym. Z pierwszej funkcji własnej oraz statystyk dwupunktowych w poprzek przepływu wyznaczone zostało przybliżone pole prędkości typowej dla obszaru przyściennego struktury wirowej.

Manuscript received December 19, 2001; accepted for print April 5, 2002